

# Performance Improvements of THz Imagers Based on Uncooled Antenna-Coupled Bolometer

J. Meilhan<sup>1</sup>, G. T. Ayenew<sup>1</sup>, L. Dussopt<sup>1</sup>, M. Hamdi<sup>2</sup>, A. Hamelin<sup>1</sup>, B. Hiberty<sup>3</sup>, J. Lalanne-Dera<sup>2</sup>, A. Minasyan<sup>3</sup>, O. Redon<sup>2</sup> and F. Simoens<sup>1</sup>

<sup>1</sup>Univ. Grenoble Alpes, CEA, LETI, MINATEC campus, Grenoble, F38054 FRANCE

<sup>2</sup>CEA Tech Nouvelle-Aquitaine, Cité de la Photonique, Pessac, 33600 France

<sup>3</sup>I2S, Pessac, 33600 France

**Abstract**—The intrinsic performance of the antenna-coupled bolometer array developed at CEA-LETI was hampered by the noise of the readout chain. Recent improvements of the camera electronics have made possible the optimization of the sensor operation in bias and integration time. It results in a real-time uncooled imager with a sensor-limited minimum detectable power that is improved by a factor of 3, i.e. close to 10 pW, at 2.5 THz.

## I. INTRODUCTION

The 320×240 antenna-coupled micro-bolometer array developed at LETI still has room for improvements in terms of Minimum Detectable Power (MDP) [1]. This performance margin is highlighted when the MDP at the imager output, previously measured close to 32 pW at 2.5 THz, is compared to the MDP of the bolometer bridge (Fig. 1). Detailed modeling [2] of the bolometer read-out showed that a MDP of 14.8 pW is reached prior to the integration stage and is degraded by the following stages.

### Imager

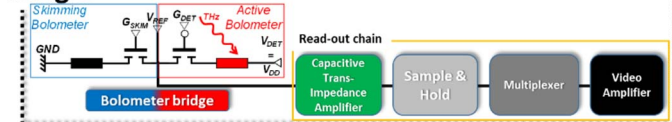


Fig. 1. Schematic of the read-out chain of the THz bolometer array

The recent integration of the sensor within a dedicated camera's electronics lowered the chain noise from 350 to 155  $\mu$ V RMS and closed the gap to the intrinsic bolometer performance with an imager MDP that now reaches 20 pW. The read-out chain noise still damps the signal to noise ratio (SNR) of the detector, but many options are available to improve the overall SNR. Thanks to a low noise design of the critical power supplies integrated within the camera electronics, the bias level of the bolometer bridge elements has been optimized in order to achieve a significant gain in terms of MDP. The sensitivity of the detector has also been boosted through the increase in integration time of the bolometer bridge current.

## II. RESULTS

The general idea that we studied is based on getting the bolometer bridge noise dominant with respect to the noise arising from the subsequent stages whereas its SNR is at least kept constant. Usually voltage bias of the bolometer is performed thanks to an injection MOSFET operated in saturation. The bias range is limited by the voltage drop at the channel which can be reduced in the conduction regime. However in this mode of operation the transconductance of the MOSFET shifts by several orders of magnitude and the equivalent admittance of the bolometer bridge is no more negligible. This leads to an increase of the op-amp and

reference voltage  $V_{REF}$  contribution to the total integrated current noise [3]. In order to estimate the impedance dependence of the bolometer bridge on the bias voltage and its consequences on the output noise, a small signal analysis of the different stages has been performed. Equivalent small-signal representation of the bolometer bridge with equivalent impedance  $Z_{IN}$  and integrated current noise  $\Delta I_n^{IN}$ , followed by the CTIA stage with input equivalent voltage noise  $\Delta V_n^{TIA}$  is illustrated on Fig. 2.

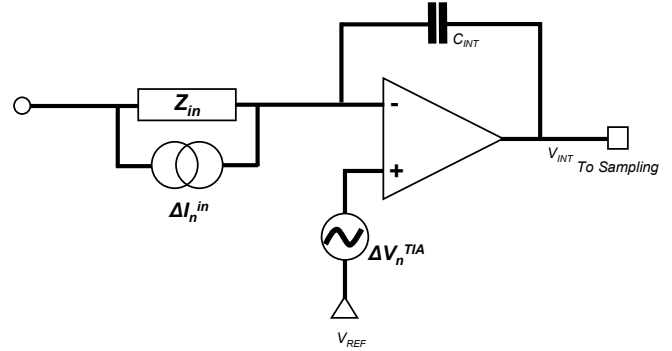


Fig. 2. Small signal representation of the bolometer bridge followed by the integration stage

Thanks to ELDO® simulations of the CTIA in follower operation, we have evaluated its input equivalent voltage noise  $\Delta V_n^{TIA}$  that leads to an input integrated current noise  $\Delta I_n^{TIA} = \Delta V_n^{TIA}/Z_{IN}$ . This noise source has been added to the previous model of the pulsed bolometer read-out [2] and resulting output noise of the imager has been estimated for different values of the grid voltage  $G_{DET}$  of the active bolometer injection MOS. Grid voltage  $G_{SKIM}$  of the skimming part was accordingly set to achieve a mid-range video output. We also assumed that thanks to an improved filtering design, the noise of the TIA voltage reference provided by the camera electronic can be neglected.

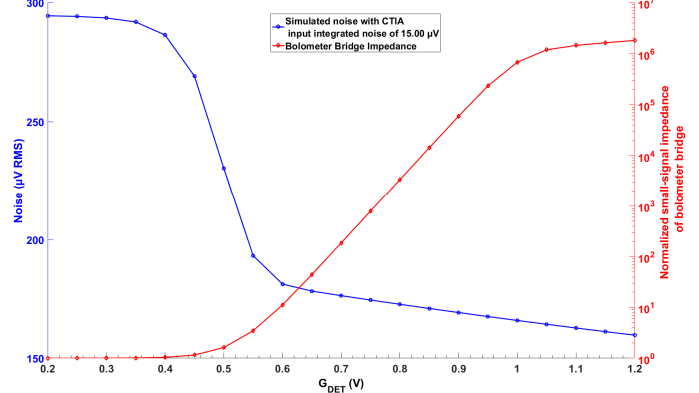


Fig. 3. Dependence on  $G_{DET}$  of the simulated video output noise and small signal impedance  $Z_{IN}$  of the bolometer bridge normalized to  $Z_{IN}$  value achieved when injection MOSFETs are operated in linear mode.

As shown on Fig. 3, for  $G_{DET}$  values above 1 V the injection MOSFETs are in the saturation regime and their conductance [4] is dominated by the residual output conductances  $g_{ds}$  while the drain transconductances  $g_{md} = \partial I_D / \partial V_D$  are negligible. In that case, the equivalent voltage of the TIA is efficiently rejected by the large impedance of the bridge and does not impact the video output noise.

As  $G_{DET}$  is decreased, the current  $I_{bol}$  within the bolometers increases. The responsivity  $\mathcal{R}_{bol} \propto I_{bol}$  is appreciated proportionally as well as the SNR since the bolometer bridge noise is dominated by the thermal noise of the bolometers.

The injection MOSFETs approach the linear regime of operation where the transconductance values become significant. The normalized impedance  $Z_{in}$  tends towards unity with a predominant contribution of the bolometer impedance and integrated current noise due to TIA  $\Delta I_n^{TIA}$  becomes gradually significant. This leads to a huge degradation of the output noise figure that will overcome the expected gain in responsivity provided by the increased current of the bolometer.

Experimental results carried out with the antenna-coupled bolometer array integrated within the I2S camera [5] have confirmed this preliminary analysis (Fig. 4).

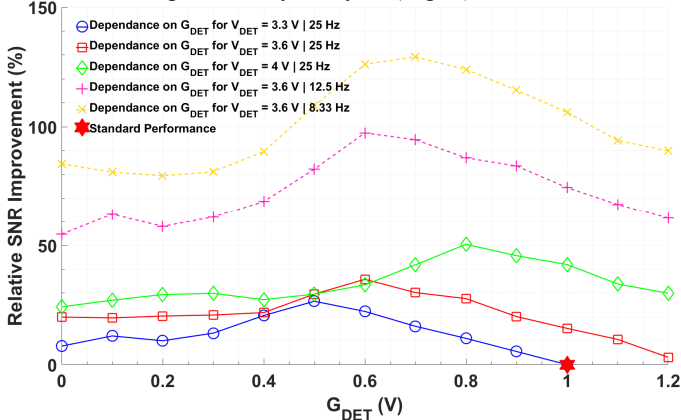


Fig. 4. Improvement of the detector SNR as a function of the bias voltage of bolometer bridge  $G_{DET}$  and  $V_{DET}$  w.r.t. to the SNR in standard bias conditions.

Compared to previous operating conditions, a MDP improvement of 27% is observed with an optimized bias ( $G_{DET} \sim 0.5$  V). The location of the SNR peak matches the grid voltage at which our model predicts an inflection point of the output noise. This result confirms the strong improvement of the supply voltage bias in terms of noise that is now negligible compare to the readout intrinsic noise.

The maximum operating voltage of the CMOS circuit can also be pushed beyond 3.3 V without notable impact on reliability. It provides a gain on bolometer bias and lifts the performances by 36% and 50% for  $V_{DET}$  pushed to 3.6 and 4 V.

Further improvement is carried out through the lengthening of the integration window ( $T_{INT}$ ) of the bolometer current. It improves the gain while reducing the frequency bandwidth of the CTIA stage. The SNR is appreciated with  $\sqrt{T_{INT}}$  as bolometer thermal noise is dominant and almost 100% of relative improvement is obtained in comparison to the initial 20 pW MDP at the cost of a frame rate reduction to 12.5 Hz. Another consequence of the frame rate reduction is the proportional increase of the readout chain gain that will hamper the imaging dynamic range.

Frame rate reduction by a factor of 3 still offers a sufficient dynamic range and achieves a 130% improvement of the SNR, i.e. a 8.45 pW MDP at 2.5 THz. As these improvements are strictly carried out thanks to the optimization of the detector and ROIC driving, a global enhancement of the MDP is obtained on the whole THz spectral range.

A concrete illustration of the advantages in terms of imaging provided by these recent developments is represented in Fig. 5. A 1 THz beam barely resolved with the chosen contrast scale appears much more clearly when the camera is switched to the optimized operating conditions. These enhancements of sensitivity are a significant leverage for the development of THz imaging system where the detection level is challenging.

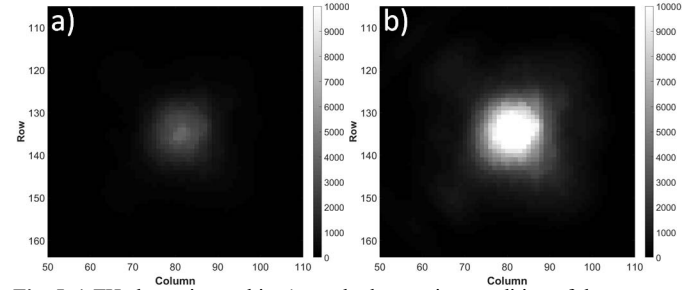


Fig. 5. 1 THz beam imaged in a) standard operating condition of the camera -  $G_{DET} = 1$  V with 25 Hz frame rate and b) optimized conditions -  $G_{DET} = 0.55$  V with 8.33 Hz frame rate.

### III. CONCLUSION

Progress in the electronic driving the CEA-Leti antenna-coupled bolometer array of the I2S camera enabled significant improvements of the sensor performances. A 8.5 pW MDP at 2.5 THz can be achieved and represents a significant step in comparison to previously reported performances.

### REFERENCES

- [1] N. Oda, I. Hosako, T. Ishii, H. Minamide, C. Otani, and N. Sekine, "The Need of Terahertz Cameras for Standardizing Sensitivity Measurements," *J. Infrared Millim. Terahertz Waves*, vol. 35, no. 8, pp. 671–685, Aug. 2014.
- [2] F. Simoens, J. Meilhan, and J.-A. Nicolas, "Terahertz Real-Time Imaging Uncooled Arrays Based on Antenna-Coupled Bolometers or FET Developed at CEA-Leti," *J. Infrared Millim. Terahertz Waves*, vol. 36, no. 10, pp. 961–985, Oct. 2015.
- [3] D. Kim, B. Goldstein, W. Tang, F. J. Sigworth, and E. Culurciello, "Noise Analysis and Performance Comparison of Low Current Measurement Systems for Biomedical Applications," *IEEE Trans. Biomed. Circuits Syst.*, vol. 7, no. 1, pp. 52–62, Feb. 2013.
- [4] C. Enz, F. Krummenacher, and E. A. Vittoz, "An analytical MOS transistor model valid in all regions of operation and dedicated to low-voltage and low-current applications," *Analog Integr. Circuits Signal Process.*, vol. 8, no. 1, pp. 83–114, Jul. 1995.
- [5] "i2s - TZcam camera." [Online]. Available: <https://www.i2s.fr/en/product/tzcam>. [Accessed: 22-Jun-2018].